Critical behavior of the square-well fluid with λ = 2: A finite-size-scaling study

Enrique de Miguel

Departamento de Física Atómica, Molecular y Nuclear, Universidad de Sevilla, Apartado 1065, Sevilla 41080, Spain

We report a Monte Carlo study of the liquid-vapor coexistence region and critical region of the square-well fluid with range parameter $\lambda = 2$. The liquid-vapor coexistence curve has been obtained by using the Gibbs ensemble Monte Carlo method and the critical parameters estimated by analyzing the resulting coexistence densities using a Wegner expansion truncated up to first-order terms. The shape of the coexistence curve in the temperature-density plane of the phase diagram has been described in terms of an effective exponent, β_e. Our results seem to indicate that the coexistence curve is well described by a nearly universal value of β_e, in contrast with previous results, where it is claimed that the coexistence curve is compatible with a mean-field value of β_e. The critical point of the system has been calculated with a higher degree of accuracy by implementing the cumulant intersection method with the help of the reweighting technique. The universality class to which this critical point belongs has been investigated implementing a mixed-field finite-size-scaling simulation study within the grand canonical ensemble. By analyzing the scaling properties of the distribution functions of the scaling operators at criticality, the Ising character of the critical point is confirmed for this system. This is further corroborated by the calculated values of the critical exponent ratios β/ν and $1/\nu$, which are compatible with the expected values for the three-dimensional Ising universality class and incompatible with the corresponding mean-field values. [S1063-651X(97)00302-4]

PACS number(s): 64.60.Fr, 64.70.Fx, 05.70.Jk

I. INTRODUCTION

It is well established [1] that close to the liquid-vapor (LV) critical point, the order parameter $(\rho_l - \rho_v)$ vanishes according to the scaling law

$$(\rho_l - \rho_v) \sim |t|^\beta, \tag{1}$$

where ρ_l and ρ_v are the liquid and vapor coexistence densities, respectively, at temperature T. Here, t is defined as $t = (T - T_c)/T_c$ with T_c being the critical temperature, and β is the (order-parameter) critical exponent. It is also generally accepted that this critical point belongs to the three-dimensional (3D) Ising universality class with a value $\beta \approx 1/3$ [1]. This implies that the LV coexistence curve is cubic in shape for $T \to T_c^-$.

Less well known is the shape of the LV coexistence curve for temperatures well below T_c. This question has been addressed by Singh and Pitzer [2] in a study of particular interest in which existing experimental data on a number of liquid-vapor systems have been reexamined. This analysis was implemented in terms of an effective exponent β_e and a Wegner expansion [3] which accounts for corrections to scaling outside the critical region.

The effective exponent β_e was first introduced by Vershaffelt [4] a century ago as a sensitive parameter to measure the shape of the LV coexistence curve. It is defined as

$$\beta_e = \frac{\partial \ln(\rho_l - \rho_v)}{\partial \ln|t|}. \tag{2}$$

As claimed by Singh and Pitzer [2], β_e is nearly constant over a wide range of temperatures for simple fluids with typical values of β_e in the range 0.33–0.36. Additionally, for

temperatures close enough to T_c, $\beta_e \to \beta$, as expected. Simulation results seem to confirm that β_e follows a similar pattern for simple fluid models. From the analysis of Panagiotopoulos's Gibbs ensemble results for the Lennard-Jones model [5], Singh and Pitzer found that β_e, for this system, is fairly constant over a temperature range $0.68 < T/T_c < 0.97$ with $\beta_e \approx 0.34$. It was finally suggested that the shape of a LV coexistence curve is never accurately described by a mean-field effective exponent ($\beta_e = 1/2$).

This point has been questioned by Vega *et al.* [6] in a subsequent simulation study of the square-well (SW) fluid model. This model constitutes the simplest fluid model including both repulsive and short-range attractive interactions and is explicitly given by

$$u(r) = \begin{cases} \infty, & \text{if } r < \sigma \\ -\epsilon, & \text{if } \sigma \leq r < \lambda\sigma \\ 0, & \text{if } r \geq \lambda\sigma, \end{cases} \tag{3}$$

where r is the distance between the centers of mass of the SW particles, σ is the diameter of the (spherical) hard core, λ is the (dimensionless) range of the potential, and ϵ is the well depth.

In Ref. [6], an extensive computer simulation study of the LV phase equilibria and critical properties of SW fluids is reported for different values of the potential range with $1.25 \leq \lambda \leq 2$. As claimed by Vega *et al.*, the results for SW fluids with $\lambda \leq 1.75$ seem to follow the general trend found by Singh and Pitzer, as the corresponding LV coexistence curves are nearly cubic in shape and are well represented by an effective exponent β_e very close to the expected universal value $\beta \approx 1/3$. Surprisingly, the results for the largest potential range considered in Ref. [6] are in stark contrast with this

generic behavior: the coexistence curve for $\lambda = 2$ was found to be nearly quadratic in shape and described by an effective exponent $\beta_e = 0.53 \pm 0.11$. Additionally, it was concluded in Ref. [6] that either the shape of the coexistence curve should change quite dramatically close enough to the critical point (so as to observe the expected $\beta_e \rightarrow \beta$ as $T \rightarrow T_c$), or even that the SW fluid with $\lambda = 2$ does not belong to the 3D Ising universality class. Although classical behavior ($\beta = 1/2$) is expected in the limit of infinite range attractive interactions, it does not seem plausible that this limit has been attained for the SW fluid with $\lambda = 2$.

The above-mentioned considerations prompted us to analyze critically the behavior of the SW fluid with $\lambda = 2$. First, the LV coexistence curve was recalculated using the Gibbs ensemble Monte Carlo (GEMC) simulation method [5,7,8] and considering larger systems than those reported previously [6] in order to check whether the results reported by Vega *et al.* were affected to some extent by system-size effects. Additionally, coexistence properties were obtained for a wider range of temperatures and, particularly, for temperatures closer to the critical point. This is expected to yield a more detailed information regarding the shape of the LV coexistence curve and the approach to the critical point for this system.

The present work was completed with an independent study of the critical properties of the SW fluid with $\lambda = 2$ within the context of finite-size scaling (FSS) simulation techniques [9]. These techniques have proven extremely powerful in obtaining the critical parameters from simulations of finite-size systems in a large variety of physical systems. In most applications, full FSS analysis has been limited to spinlike models with the Ising symmetry [9]. More recently, Wilding and Bruce [10,11] have extended these ideas to the study of critical properties of fluids with reduced symmetry incorporating explicitly the effects of field mixing. The success of this extended mixed-field FSS theory has been convincingly demonstrated in the study of the critical behavior of the two-dimensional (2D) and 3D Lennard-Jones fluid [10–12], 2D and 3D asymmetric lattice gas model [13,14], and polymer mixtures [15].

The remainder of the paper is organized as follows. In Sec. II we give details of the simulations performed for the SW fluid with $\lambda = 2$ using the GEMC method. The LV coexistence properties for this system are then presented and discussed for the two system sizes investigated in the present work. In this section we also give details of the extrapolation procedure used to obtain a first estimate of the critical constants of the system. The overall shape of the coexistence curve, as measured from the effective exponent β_e, is also studied and comparison is made with previous results [6].

In Sec. III, a brief survey is given of the basic ideas underlying the field-mixing FSS techniques [10,11] as applied to the simulation of critical phenomena in fluid systems. We then turn to the application of these ideas to the simulation of the critical region of the SW fluid with $\lambda = 2$. The critical point is located by using the cumulant intersection method [16] with the aid of histogram reweighting techniques [17] within the grand canonical ensemble. We then analyze the scaling properties of the distribution functions of suitable scaling variables, which in turn, allow us to determine the

universality class to which the critical point of the system belongs. Finally, our results are summarized in Sec. IV.

II. GIBBS ENSEMBLE SIMULATION RESULTS

The Gibbs ensemble Monte Carlo method [5,7,8] is one of the most widely used techniques to study fluid phase equilibria from computer simulation. The reader is referred to the original papers [5,7] and to a recent review [8] for details regarding the practical implementation of the method. In the present work, the LV coexistence properties of the SW fluid with $\lambda = 2$ were investigated by using the GEMC technique.

A first set of simulations was performed for systems containing $N = 756$ particles. In most cases, the initial vapor and liquid configurations were generated by placing 256 and 500 particles, respectively, on a fcc lattice. For some temperatures, the starting configuration was taken from the final (equilibrated) configuration corresponding to a different temperature. The initial configuration was equilibrated in all instances for at least 5×10^4 cycles, each cycle corresponding to N particle displacements, one volume change attempt, and N_t attempts to transfer a particle from one phase to the other. N_t typically varied from 750 (for the lower temperatures) to 40 (for near-critical temperatures). The value of N_t at each temperature was chosen so as to obtain equal chemical potential values in both subsystems at equilibrium. Averages for the properties of the two coexisting phases were calculated over 1×10^5 additional cycles. For temperatures close to the critical point, longer runs implying $2-3 \times 10^5$ cycles were performed.

The coexisting densities for temperatures within the range $2.25 \leqslant T \leqslant 2.63$ are included in Table I. The temperature is expressed in units of ϵ / k_B and the particle density in units of σ^{-3}. For temperatures $T < 2.60$, both subsystems kept their initial (vapor or liquid) identity during the simulations. In such cases, the coexistence values were obtained by averaging over blocks of 1000 cycles. At higher temperatures, however, both subsystems were observed to switch identity, as expected for temperatures sufficiently close to the critical temperature. For these temperatures, results were analyzed in terms of histograms of the relative frequency of the particle density. The corresponding coexistence densities were thus associated to the position of the peaks in the density histograms and standard deviations with the width of the corresponding peaks.

In order to check possible system-size effects on the calculated coexistence properties, a second set of simulations was performed considering larger systems consisting on $N = 1364$ SW particles. The initial vapor and liquid configurations were generated in a similar way, by considering 500 and 864 particles, respectively, on a fcc lattice. The coexistence densities for temperatures in the range $0.245 \leqslant T \leqslant 0.263$ are included in Table I.

The liquid-vapor coexistence curve is shown in Fig. 1 in the temperature-density projection of the phase diagram for the two system sizes investigated in this work. No system-size effects were observed within the statistical accuracy of our results. The results obtained by Vega *et al.* [6] for systems with $N = 512$ SW particles are also shown in the figure for comparison. According to Fig. 1, there is a slight (but appreciable) difference between the results obtained with

TABLE I. Liquid (ρ_l) and vapor (ρ_v) coexistence densities obtained from Gibbs ensemble Monte Carlo simulations of systems with $N=756$ and $N=1364$ SW particles with a potential range $\lambda=2$. The temperature (T) is expressed in units of ϵ/k_B and the densities (ρ_l, and ρ_v) are expressed in units of σ^{-3}.

T	N=756		N=1364	
	ρ_v	ρ_l	ρ_v	ρ_l
2.63	0.131(14)	0.364(33)	0.126(8)	0.367(28)
2.62	0.120(16)	0.361(45)	0.118(10)	0.362(26)
2.61	0.110(22)	0.370(36)	0.116(9)	0.371(19)
2.60	0.104(14)	0.376(18)	0.112(7)	0.378(16)
2.58	0.105(7)	0.392(18)	0.107(5)	0.413(13)
2.56	0.104(6)	0.429(11)	0.101(6)	0.426(12)
2.54	0.098(5)	0.442(8)	0.094(5)	0.433(10)
2.52	0.091(4)	0.452(9)	0.087(4)	0.443(10)
2.50	0.084(5)	0.462(9)	0.079(4)	0.447(10)
2.45	0.072(3)	0.489(9)	0.074(2)	0.485(8)
2.40	0.064(2)	0.514(8)		
2.35	0.056(2)	0.538(7)		
2.30	0.057(2)	0.575(7)		
2.25	0.040(2)	0.574(6)		

$N=512$ and those obtained in the present work. These differences are attributed to an unsufficient equilibration of the simulations reported in Ref. [6] and not to system-size effects [18].

The liquid-vapor data can be used to estimate the location of the critical point. A careful analysis would, in principle, involve the use of several terms in the general Wegner expansion of the order parameter ($\rho_l-\rho_v$), and in the expansion of the ''diameters'' of the coexistence curve, ($\rho_l+\rho_v$)/2. However, the Gibbs ensemble data included in Table I are not of sufficient precision for a highly accurate analysis. According to this, and in line with related works,

we decided to keep only the leading terms in the general Wegner expansions. In practice, the critical temperature, T_c, and the critical density, ρ_c, were obtained by fitting the simulation data to

$$\frac{\rho_l+\rho_v}{2}=\rho_c+C_2|t|, \qquad (4)$$

$$\rho_l-\rho_v=B_0|t|^\beta, \qquad (5)$$

where B_0 and C_2 are the coefficients of the leading terms in the general Wegner expansions and β is the critical exponent.

Equation (4) is the so-called law of rectilinear diameters and its use is justified considering that the anomaly in the diameter of the coexistence curve close to the critical point is normally very weak and difficult to observe.

Use of Eq. (5) for evaluating T_c using temperatures well below the critical region should be regarded with some care. In principle, Eq. (5) is just an asymptotic relation and its validity is limited to data sufficiently close to T_c. It is normal practice, however, to fix β in Eq. (5) to the appropriate critical exponent and estimate T_c by fitting the simulation data over the entire range of temperatures. This procedure yields a fairly good estimate of T_c for systems in which the effective exponent defined in Eq. (2) is nearly constant over the considered range of temperatures.

A different possibility implies considering β in Eq. (5) as an additional adjustable parameter. This free parameter coincides with β_e for systems with a temperature-independent effective exponent. Under this assumption, Vega et al. [6] used Eq. (5) with $\beta=\beta_e$ to describe the shape of the coexistence curve for the SW fluid with variable λ. As claimed in Ref. [6], the LV coexistence curves for systems with $1.25\leq\lambda\leq1.75$ were well described by an exponent close to the universal value, while for $\lambda=2$ the best fit was obtained for the value $\beta_e=0.53\pm0.11$.
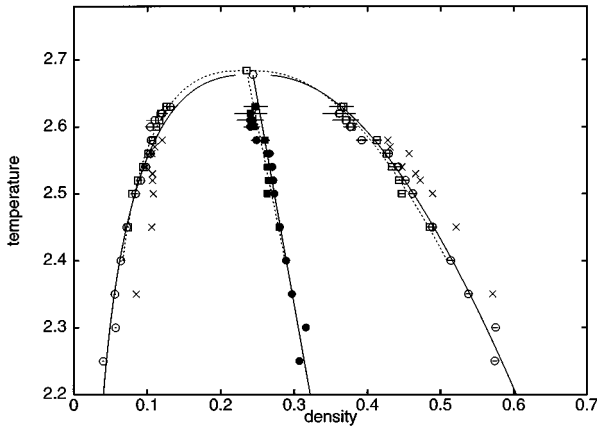
FIG. 1. Temperature-density liquid-vapor coexistence curve for the square-well fluid with $\lambda=2$ as obtained from Gibbs ensemble Monte Carlo simulation for systems with $N=756$ particles (dots) and $N=1364$ particles (squares). Open symbols are for the vapor ρ_v and liquid ρ_l coexistence densities; filled symbols are for the diameters ($\rho_l+\rho_v$)/2. The crosses correspond to the results from Ref. [6]. The lines are obtained by fitting the simulation data for $N=756$ (solid line) and $N=1364$ (dashed line) to Eqs. (4) and (5). The estimated location of the critical point for each N is also shown in the figure. The temperature is in units of (ϵ/k_B) and the density is in units of σ^{-3}.

TABLE II. Values of the critical temperature T_c, critical density ρ_c, and coefficients B_0 and C_2 as obtained from fitting the Gibbs ensemble Monte Carlo simulation results for systems with N SW particles with $\lambda = 2$ included in Table I to Eqs. (4) and (5). Results for $N = 756$ and 1364 correspond to the present work. Also included are the results obtained for $N = 512$ by Vega *et al.* [6]. Results labeled † were obtained by considering the effective exponent β_e as a free parameter, and the remainder by fixing β_e to 1/3 or 1/2.

N	β_e	T_c	ρ_c	B_0	C_2
512	$0.54(11)^\dagger$	2.764(23)	0.225(18)	1.31(12)	0.72(8)
756	$0.40(5)^\dagger$	2.678(27)	0.244(8)	1.12(9)	0.44(7)
	1/3	2.648(14)	0.249(8)	1.00(12)	0.43(7)
	1/2	2.730(14)	0.235(8)	1.29(22)	0.45(7)
1364	$0.39(15)^\dagger$	2.684(51)	0.235(82)	1.06(33)	0.50(21)
	1/3	2.666(85)	0.238(81)	0.94(40)	0.49(21)
	1/2	2.721(89)	0.228(85)	1.31(36)	0.50(21)

We have included in Table II the critical parameters obtained after fitting our Gibbs ensemble data for systems with $N = 756$ and 1364 particles to Eqs. (4) and (5) with $\beta = \beta_e$ left as a free parameter. For both system sizes, the LV curves were well represented by a substantially lower effective exponent than that reported in Ref. [6]. For systems with $N = 756$ we found $\beta_e = 0.40 \pm 0.05$ and for systems with $N = 1364$ we found $\beta_e = 0.39 \pm 0.15$.

We have also obtained the critical parameters by fixing the exponent β in Eq. (5) to $\beta = 1/3$ and $\beta = 1/2$. The corresponding values are included in Table II.

From these results it seems plausible to conclude that the shape of the coexistence curve for the SW fluid with $\lambda = 2$ is nearly cubic and is not accurately described by a mean-field effective exponent.

The question of whether the coexistence curve closes at T_c in a mean-field or universal fashion (i.e., whether $\beta_e \to 1/2$ or 1/3 as $T \to T_c$) still remains unresolved and is addressed in Sec. III.

III. FINITE-SIZE SCALING

One of the potential uses of FSS techniques is to investigate critical phenomena from numerical computer simulations performed in small samples [9]. The most widely used approach exploits the scaling properties of the order-parameter distribution function [16]. The prediction that the form of this distribution at the critical point is unique for all members of a given universality class has been largely supported from computer simulation [9].

Only recently have these techniques been generalized to deal with simulation of critical behavior in liquids lacking the Ising symmetry. In this context, Wilding and Bruce have developed a FSS theory incorporating the effects of field mixing [10,11]. This approach has been tested and its implications analyzed for a number of systems in a surprisingly successful way [10–15].

In the following subsection, we highlight some of the ideas underlying the mixed-field FSS theory which are of relevance for the present work.

A. Theoretical details

We consider a classical fluid system in a volume $V = L^d$, where d is the dimensionality of the system, described in the

grand canonical ensemble. The (particle) density will be denoted as $\rho = N/V$ and the energy density by $u = U/V$, where U is the configurational energy of the system.

Let $p_L(\rho, u)$ be the probability distribution function of density and energy fluctuations for a system of linear dimension L for given thermodynamic conditions specified by the dimensionless (inverse) temperature $\bar{\beta} = \epsilon/(k_B T)$, and the dimensionless chemical potential $\bar{\mu} = \mu/(k_B T)$. Here, k_B is Boltzmann's constant and ϵ is the energy scale of the system. This distribution can be formally written as an ensemble average and is readily accessible from a computer simulation.

It is well established [19] that the behavior of the system close to the critical point is controlled by two relevant scaling fields, namely, the thermal scaling field τ and the ordering scaling field h. These scaling fields are analytic functions of the chemical potential and temperature and vanish identically at the critical point. In the critical region, τ and h can be expressed as combinations of the deviations of $\bar{\mu}$ and $\bar{\beta}$ from their critical values, $\bar{\mu}_c$ and $\bar{\beta}_c$. Specifically, and to linear-order terms, it is expected [19]

$$\tau = \bar{\beta}_c - \bar{\beta} + s(\bar{\mu} - \bar{\mu}_c), \tag{6}$$

$$h = \bar{\mu} - \bar{\mu}_c + r(\bar{\beta}_c - \bar{\beta}), \tag{7}$$

where s and r are nonuniversal parameters which accounts for the degree of field mixing [10,11].

From the scaling fields τ and h two (conjugate) scaling operators M and E are defined by requiring [10,11]

$$\langle E \rangle = \frac{1}{V}\left(\frac{\partial \ln Q_L}{\partial \tau} \right), \tag{8}$$

$$\langle M \rangle = \frac{1}{V}\left(\frac{\partial \ln Q_L}{\partial h} \right), \tag{9}$$

where Q_L denotes the grand canonical partition function for a system of linear dimension L and the brackets indicate an average over this ensemble.

Following the above convention, the scaling operators M and E can be explicitly written as a combination (or *mixing*) of the particle density and energy density

$$M = \frac{1}{1-sr}(\rho - su), \qquad (10)$$

$$E = \frac{1}{1-sr}(u - r\rho), \qquad (11)$$

According to these expressions, the distribution of mixed operators, $p_L(M,E)$ is related to $p_L(\rho,u)$ by

$$p_L(M,E) = (1-sr)p_L(\rho,u). \qquad (12)$$

Close to the critical point, and for sufficiently large system sizes, the distribution functions $p_L(M) = \int dE p_L(M,E)$ and $p_L(E) = \int dM p_L(M,E)$ of the single operators are expected to be expressed in terms of scaling relations of the form [10,11]

$$p_L(M) \approx a_M^{-1} L^{\beta/\nu} \widetilde{p}_M(a_M^{-1} L^{\beta/\nu} \delta M, a_M L^{d-\beta/\nu} h, a_E L^{1/\nu}\tau), \qquad (13)$$

$$p_L(E) \approx a_E^{-1} L^{d-1/\nu} \widetilde{p}_E(a_E^{-1} L^{d-1/\nu} \delta E, a_M L^{d-\beta/\nu} h, a_E L^{1/\nu}\tau). \qquad (14)$$

Here, δM and δE are given by $\delta M = M - M_c$ and $\delta E = E - E_c$, where M_c and E_c denote average values at criticality. The functions $\widetilde{p}_M$ and $\widetilde{p}_E$ are expected to be universal under appropriate choices of the metric factors a_M and a_E of the corresponding scaling fields. Relations (13) and (14) constitute the basic scaling postulates. Exactly at the critical point, the scaling fields vanish and, from Eqs. (13) and (14), it follows:

$$p_L(M) \approx a_M^{-1} L^{\beta/\nu} \widetilde{p}_M^*(a_M^{-1} L^{\beta/\nu} \delta M), \qquad (15)$$

$$p_L(E) \approx a_E^{-1} L^{d-1/\nu} \widetilde{p}_E^*(a_E^{-1} L^{d-1/\nu} \delta E), \qquad (16)$$

where $\widetilde{p}_M^*(x)$ and $\widetilde{p}_E^*(y)$ are universal functions of the scaling variables $x = a_M^{-1} L^{\beta/\nu} \delta M$ and $y = a_E^{-1} L^{d-1/\nu} \delta E$, respectively, and correspond to the fixed-point distributions which describe each universality class.

In most applications of mixed-field FSS techniques, the universality class is assumed (or known beforehand). Having then an independent evaluation of the corresponding fixed-point functions $\widetilde{p}_M^*(x)$ and $\widetilde{p}_E^*(y)$ allows the determination of the critical point by requiring that $p_L(M)$ and $p_L(E)$ collapse onto the respective fixed-point functions.

We did not follow this procedure, as the determination of the universality class is one the objectives of the present study. Instead, the critical point was independently evaluated (see below). According to Eqs. (15) and (16), $p_L(M)$ and $p_L(E)$ for different system sizes should become independent of L at the calculated critical point. The particular form of these single, system-size independent curves constitutes an unambiguous signature of the corresponding universality class.

It is important to recall at this point that all these conclusions only apply in the limit of large L in which correction-to-scaling effects are expected to be negligibly small [10,11].

B. FSS study of the SW fluid

The critical region of the SW fluid with $\lambda = 2$ was explored using Monte Carlo simulations in the grand canonical ensemble. Several system sizes, corresponding to volumes $V = 800, 1500,$ and 2500 (in σ^3 units) were investigated. The simulation box was cubic and usual periodic boundary conditions were used. The initial configuration was generated by considering 256 (for $V = 800$), 500 (for $V = 1500$), and 864 (for $V = 2500$) particles on the sites of a fcc lattice.

For given values of the chemical potential $\bar{\mu}$ and temperature T, this starting configuration was allowed to relax to equilibrium by performing particle displacements and insertion-deletion of particles according to well established Monte Carlo acceptance-rejection rules [20]. Typically, this initial equilibration stage consisted on 3×10^5 cycles, each cycle comprising N particle displacements (where N is the instantaneous number of particles) and 50 particle insertion-deletion attempts.

The key observable in our simulations was the distribution function of particle density and energy density fluctuations $p_L(\rho,u)$, defined previously. Once equilibrium was reached this quantity was measured as a double histogram. Rather long simulations are required in order to obtain a reliable sampling of $p_L(\rho,u)$. With the aim of saving computational time, successive configurations were generated by implementing just the particle insertion-deletion step, and no explicit particle displacements were performed during the production stage of the simulation. As claimed by Wilding and Bruce [10,11], this restricted implementation of the usual grand canonical ensemble Monte Carlo scheme is justified, as the density fluctuations are correctly sampled. On the other hand, particle displacements are performed implicitly as a result of the particle insertion-deletion step.

The double histogram $p_L(\rho,u)$ was recorded by generating 12.5×10^7 (for $V = 800$), 25×10^7 (for $V = 1500$), and 50×10^7 (for $V = 2500$) of such configurations. These simulations were performed on a DEC Alpha 3000 workstation and required, approximately, 12, 34, and 90 hours of CPU time, respectively.

The probability distribution function $p_L(\rho,u)$ was calculated at the reference thermodynamic state $\bar{\mu}_0 = -3.0394$ and $T_0 = 2.665$. We then made use of the reweighting technique [17], which affords calculation of $p_L(\rho,u)$ at different conditions $(\bar{\mu}, T)$ in the neighborhood of the reference state point. Precisely in this region (close to the critical point), this technique is quite powerful due to the large critical fluctuations which, in turn, allow for a reliable sampling of $p_L(\rho,u)$.

The coexistence line in the $\bar{\mu}$-T plane was calculated in the neighborhood of $(\bar{\mu}_0, T_0)$ using the equal-weight criterion for the density distribution function [21], obtained from $p_L(\rho,u)$ as

$$p_L(\rho) = \int du \, p_L(\rho,u). \qquad (17)$$

For a given temperature, the value of the chemical potential at coexistence was found by reweighting $p_L(\rho)$ until the
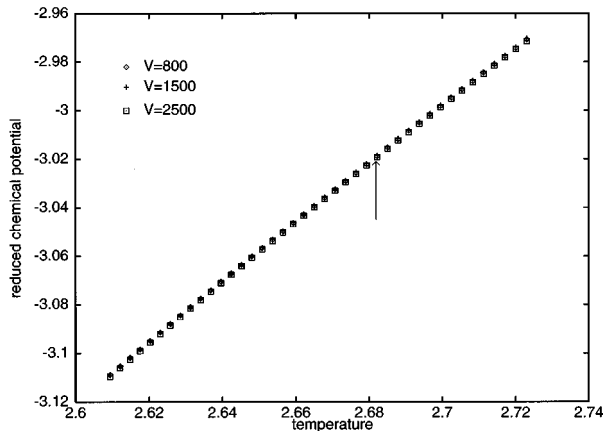
FIG. 2. Liquid-vapor coexistence line in the $\bar{\mu}$-T plane as obtained from the equal-weight criterion for three systems of volume V. The reduced chemical potential is defined as $\bar{\mu}=\mu/(k_B T)$, the temperature is in units of ϵ/k_B and the volume is in units of σ^3. The arrow indicates the location of the critical point of the system.

area enclosed by the vapor and liquid peaks appearing in $p_L(\rho)$ becomes equal.

We present in Fig. 2 the coexistence line in the $\bar{\mu}$-T plane as obtained from the equal-weight criterion for the three system sizes studied in the present work. We also show in this figure the location of the critical point (see below). One of the effects of simulating finite-size systems is that the apparent (finite-size) critical temperature is shifted to higher temperature values when compared with the true (infinite-size) critical temperature [16]. This results in the observation of a double-peak structure in $p_L(\rho)$ even above the critical temperature of the system. This effect becomes noticeable in Fig. 2, where it can be observed that the coexistence line extends for temperatures above T_c.

The critical point of the system was located as follows. For each value of V, we calculated the fourth-order Binder's cumulant, U_L, defined as [16]

$$U_L = 1 - \frac{\langle m^4 \rangle}{3 \langle m^2 \rangle^2}, \qquad (18)$$

where $m = \rho - \langle \rho \rangle$. Again, the histogram extrapolation method [17] was used to evaluate U_L as a function of temperature in the neighborhood of the reference thermodynamic state. The critical point coincides with the point at which U_L becomes system-size independent [16].

The values of U_L for system sizes corresponding to $V=800$, 1500, and 2500 are shown in Fig. 3 as a function of the temperature. According to Fig. 3, the curves intersect at a temperature value $T_c=2.6821(8)$ which corresponds to $\bar{\mu}_c=-3.019(1)$.

The universality class associated to the critical point in the SW fluid with $\lambda=2$ was independently assessed by probing the scaling behavior of the single scaling operator distributions $p_L(M)$ and $p_L(E)$. According to Eqs. (15) and (16), these distributions are predicted to collapse into single curves which, in turn, characterize the appropriate universality class. Following the definitions of the operators M and
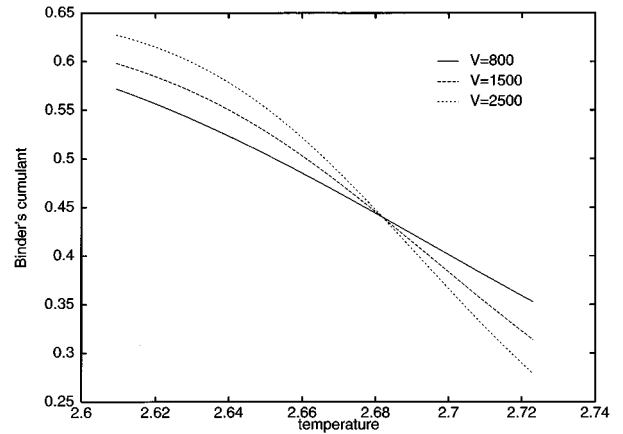
FIG. 3. The values of Binder's cumulant U_L defined in Eq. (18) as a function of temperature for different systems of volume V (in σ^3 units) and calculated along the liquid-vapor coexistence line. The intersection, which defines the location of the critical point, occurs for $T_c=2.6821(8)$ and $\bar{\mu}_c=-3.019(1)$. The temperature is in units of ϵ/k_B.

E given in Eqs. (10) and (11), this mapping requires prior knowledge of the field-mixing parameters s and r.

In practice, the value of s was found by reweighting $p_L(M)$ at the calculated values of T_c and $\bar{\mu}_c$ for each value of L until a single, system-size independent curve was found. This is illustrated in Fig. 4, where the critical ordering operator distributions are shown in terms of the scaling variable $x=a_M^{-1} L^{\beta/\nu}(M-M_c)$. The scale factor is fixed by choosing the distributions, for all system sizes, to have unit variance. The collapse of the data was effected by choosing $s=-0.01(1)$.

Similarly, the value of the parameter r was chosen by reweighting $p_L(E)$ at $(\bar{\mu}_c, T_c)$ until the curves for different system sizes collapsed onto a single, system-size independent curve. The scaling behavior of $p_L(E)$ predicted by Eq. (16) is demonstrated in Fig. 5 for the choice $r=-8.60(6)$.

A comparison of the scaling behavior of $p_L(M)$ and
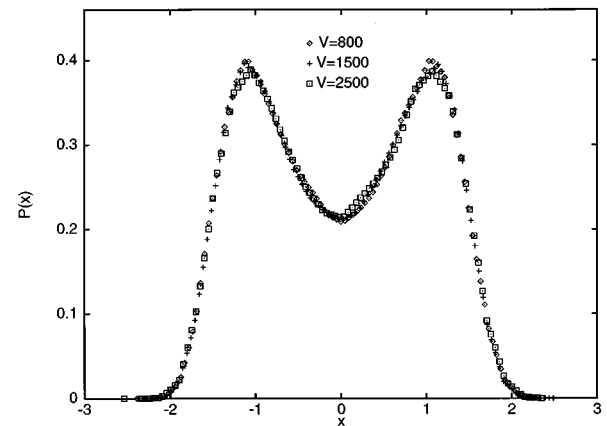
FIG. 4. The distribution functions of the scaling operator M at criticality for systems with volume $V=800$, 1500, and 2500 (in σ^3 units) as a function of the scaling variable $x=a_M^{-1} L^{\beta/\nu}(M-M_c)$. The metric factor has been chosen so that the distributions have unit variance. The matching is effected by choosing the mixing parameter $s=-0.01(1)$.
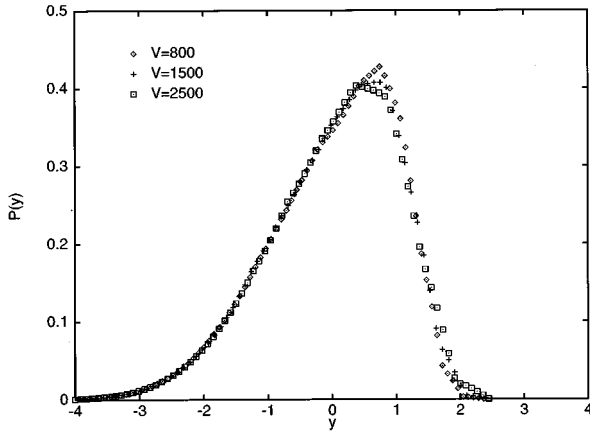
FIG. 5. The distribution functions of the scaling operator E at criticality for systems with volume $V = 800$, 1500, and 2500 (in σ^3 units) as a function of the scaling variable $y = a_E^{-1} L^{d-1/\nu}(E - E_c)$. The metric factor has been chosen so that the distributions have unit variance. The matching is effected by choosing the mixing parameter $r = -8.60(6)$.

$p_L(E)$ at criticality shown in Figs. 4 and 5 with the expected fixed-point distributions $\tilde{p}_M^*(x)$ and $\tilde{p}_E^*(y)$, for the 3D Ising model (see, for instance, Figs. 6 and 8 from Ref. [15]), permits us to conclude that the LV critical point for the SW fluid with $\lambda = 2$ belongs to the 3D Ising universality class.

It is important to recall that the distribution functions appearing in Figs. 4 and 5 have been plotted with no assumption on the values of the critical exponents β/ν and $1/\nu$. Moreover, the exponent ratios may be obtained by comparing the standard deviations of $p_L(M)$ and $p_L(E)$ as a function of system size [10,12]. We carried out this comparison for the two largest system sizes considered in this work, obtaining the values $\beta/\nu = 0.55(3)$ and $1/\nu = 1.68(6)$. These values are only in moderate agreement with the corresponding exponent ratio values obtained by Ferrenberg and Landau [22] for the 3D Ising model [$\beta/\nu = 0.518(7)$ and $1/\nu = 1.594(4)$]. Although corrections to scaling may be appreciable for the relatively small samples simulated in this work, we believe that the discrepancies between the calculated and the expected exponent ratios arise essentially from the somewhat poor statistics of the measured joint distribution functions for the larger system sizes and the errors in the location of the critical point.

IV. SUMMARY

We have presented in this work a simulation study of the LV coexistence curve and critical region of the SW fluid model with $\lambda = 2$. The LV coexistence curve has been studied by using the standard GEMC method for two system sizes. Within the accuracy of our results, the resulting vapor and liquid densities do not exhibit appreciable system-size effects over the range of temperatures covered in the present study.

The approach to criticality has been analyzed in terms of the effective critical exponent, β_e, which constitutes an indication of the shape of the LV curve. For both system sizes,

our results are consistent with a nearly universal effective exponent. This is in contrast with previous results, where it is claimed that the LV curve for this system is compatible with a mean-field effective exponent. The critical parameters have been obtained, as a first approximation, by fitting the GEMC data using a Wegner expansion including only the leading terms. The critical temperature so obtained is slightly lower than that reported previously [6].

As a more precise route for obtaining the critical point of the system, we have used the fourth-order Binder's cumulant method. With the help of the reweighting technique, we have obtained the density distribution function in the neighborhood of the critical point for three system sizes. These cumulants intersect at a well defined point defining the critical point. It has been found that $\bar{\mu}_c = -3.019(1)$ (in units of $k_B T$), and $T_c = 2.6821(8)$ (in units of ϵ/k_B). The values of the critical temperature obtained by extrapolation of the Gibbs ensemble data are $T_c = 2.678(27)$ (for $N = 756$ particles) and $T_c = 2.684(51)$ (for $N = 1364$ particles). As in the case of the Lennard-Jones model, the estimate of the critical point by using the GEMC method is rather satisfactory. We should stress that these values of the critical temperatures have been obtained by considering β as an adjustable parameter. Had this exponent been fixed to $\beta = 1/3$ (as done in most applications), the results would have been slightly different. From the data obtained in this work, fixing $\beta = 1/3$ yields $T_c = 2.648(14)$ ($N = 756$), and $T_c = 2.666(85)$ ($N = 1364$).

The neighborhood of the critical region has been explored by performing a finite-size-scaling analysis within the framework of the mixed-field FSS theory introduced by Wilding and Bruce. Our major concern at this point has been to give numerical evidence regarding the universality class to which the LV critical point for the SW fluid with $\lambda = 2$ belongs. Although it is expected that the LV critical point in fluids characterized by short-range interactions belongs to the Ising universality class, the results for $\lambda = 2$ included in Ref. [6] cast some doubts in this regard. We have shown that the distribution functions of the scaling operators at criticality for the SW fluid with $\lambda = 2$ resemble quite closely those previously reported for the 3D Ising magnet fluid, thus giving strong evidence that the SW fluid with $\lambda = 2$ belongs to the 3D Ising universality class. This is further corroborated, in part, by the values of the critical exponents obtained from our FSS analysis [$\beta/\nu = 0.55(3)$ and $1/\nu = 1.68(6)$]. Even though affected by a substantial uncertainty, our estimates for the exponent ratios β/ν and $1/\nu$ are in reasonable agreement with the values expected for the 3D Ising universality class [$\beta/\nu = 0.518(7)$ and $1/\nu = 1.594(4)$], and are incompatible with the corresponding mean-field values ($\beta/\nu = 1$ and $1/\nu = 2$).

[1] See, for instance, J.J. Pinney, N.J. Dowrick, A.J. Fisher, and M.E.J. Newman, *The Theory of Critical Phenomena* (Clarendon, Oxford, 1992).

[2] R.R. Singh and K.S. Pitzer, J. Chem. Phys. **90**, 5742 (1989).

[3] F. Wegner, Phys. Rev. B **5**, 4529 (1972).

[4] J. Vershaffelt, Commun. Lab. Phys. Univ. Leiden **28**, 1 (1896).

[5] A.Z. Panagiotopoulos, Mol. Phys. **61**, 813 (1987).

[6] L. Vega, E. de Miguel, L.F. Rull, G. Jackson, and I.A. McLure, J. Chem. Phys. **96**, 2296 (1992).

[7] A. Z. Panagiotopoulos, N. Quirke, M. Stapleton, and D.J. Tildesley, Mol. Phys. **63**, 527 (1988).

[8] A.Z. Panagiotopoulos, in *Observation, Prediction and Simulation of Phase Transitions in Complex Fluids*, Vol. 460 of *NATO Advanced Study Institute, Series C: Mathematical and Physical Sciences*, edited by M. Baus, L.F. Rull, and J.-P. Ryckaert (Kluwer, Dordrecht 1995), pp. 463–501.

[9] For a review, see *Finite Size Scaling and Numerical Simulation of Statistical Systems*, edited by V. Privman (World Scientific, Singapore, 1990).

[10] N.B. Wilding and A.D. Bruce, J. Phys. Condens. Matter **4**, 3087 (1992).

[11] A.D. Bruce and N.B. Wilding, Phys. Rev. Lett. **68**, 193 (1992).

[12] N.B. Wilding, Phys. Rev. E **52**, 602 (1995).

[13] N.B. Wilding, Z. Phys. B **93**, 119 (1993).

[14] N.B. Wilding and M. Müller, J. Chem. Phys. **102**, 2562 (1995).

[15] M. Müller and N.B. Wilding, Phys. Rev. E **51**, 2079 (1995).

[16] K. Binder, Z. Phys. B **43**, 119 (1981).

[17] A.M. Ferrenberg and R.H. Swendsen, Phys. Rev. Lett. **61**, 2635 (1988); **63**, 1195 (1989); R.H. Swendsen, Physica A **194**, 53 (1993).

[18] L. Vega (private communication).

[19] J.J. Rehr and N.D. Mermin, Phys. Rev. A **8**, 472 (1973).

[20] M.P. Allen and D.J. Tildesley, *Computer Simulation of Liquids* (Clarendon, Oxford, 1987).

[21] C. Borgs and Kotecky, J. Stat. Phys. **60**, 79 (1990).

[22] A.M. Ferrenberg and D.P. Landau, Phys. Rev. B **44**, 5081 (1991).